



Stability of liquid crystal micro-droplets based optical microresonators

Junaid Ahmad Sofi and Surajit Dhara 

School of Physics, University of Hyderabad, Hyderabad, India

ABSTRACT

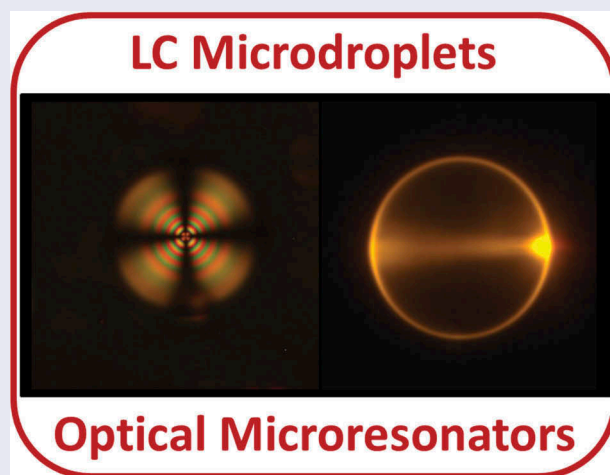
Liquid crystal (LC) based tuneable optical microresonators are potential for being used as crucial components in photonic devices. In this article, we report experimental studies on LC micro-droplets dispersed in several dispersing media. We find that the size of the micro-droplets formed in a low refractive index and optically transparent perfluoropolymer are most stable with time than commonly used dispersing media. Using a negative dielectric anisotropy nematic liquid crystal, we show that the whispering gallery mode optical resonance properties such as the quality factor and the free spectral range of stable micro-droplets are independent of the strength of the applied electric field. The optical resonance properties under applied field are significantly different than that of the liquid crystals with positive dielectric anisotropy and are explained based on the elastic deformation of the micro-droplets.

ARTICLE HISTORY

Received 5 July 2018
Accepted 21 August 2018

KEYWORDS

Liquid crystal micro-droplets; optical resonance



1. Introduction

In polymer dispersed liquid crystals, appropriate amount of polymers and liquid crystals are mixed. In the immiscible mixture, tiny droplets ranging from a few tens of nanometre to micrometre size liquid crystal droplets are phase separated from the polymer matrix [1–4]. These micro-droplets highly scatter incident light giving the sample a milky appearance. The application of electric field reorients the director (the average direction of molecular long axis [5]) of the micro-droplets and, hence, changes the scattering intensity and, thus, have been used in many applications. The dispersed droplets exhibit variety of director structure depending on the bulk elasticity, surface tension and surface anchoring. It has been shown that for sufficiently large droplets, the surface anchoring prevails. As a

result, topological defects are stable at the equilibrium states of the large droplets [6]. In addition to this, it has also been reported that both flexoelectricity and order electricity has significant effect on the equilibrium defect structure [7]. In case of nematic, if the surface anchoring is strongly homeotropic, commonly a radial director structure with a hedgehog defect at the centre of the droplets is observed. In case of strongly planar surface anchoring two boojums at the interface are usually observed. A variety of other complex structures can be observed in cholesteric and smectic-C liquid crystal micro-droplets [8–11].

Liquid crystal micro-droplets can be used as optical micro-cavities when the refractive index of the surrounding medium is lower [12–15]. The light inside the droplet circulates due to the total internal reflection and the resonance condition is achieved when the

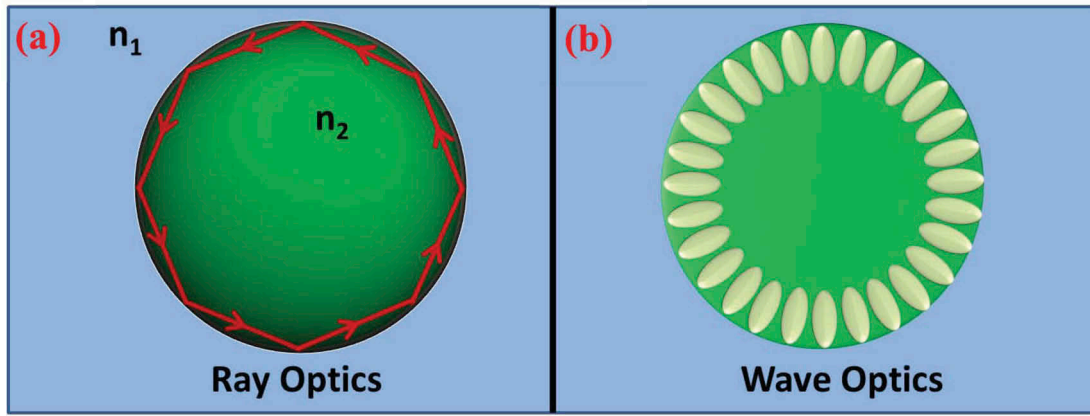


Figure 1. (Colour online) (a) Schematic diagram showing the WGM resonance of a spherical microresonator using ray and wave optics. n_1 and n_2 are the refractive indices of the respective media. (b) Small ellipsoids represent the electric field distribution of resonant modes.

circulating light meets in-phase. This is known as whispering-gallery-mode (WGM) resonance [16,17]. A schematic representation of WGM resonance using ray-optics and wave optics is shown in Figure 1. It has created a lot of interest as these micro-cavities possess a small mode volume and high quality factors (Q) and they are promising for many applications such as laser sources, active filters and all-optical switches.

The Q -factor of a spherical micro-cavity strongly depends on the morphology and the optical properties of the microsphere. In case of soft microresonators like liquid crystals they can be changed easily by varying the temperature, external electric and magnetic fields. The evanescent field that exists up to a few hundreds of nanometres and lies outside the micro-cavity makes these tiny resonators efficient sensors. Any modulation in the evanescent field domain of these droplets is strongly reflected in their optical resonance. Based on this, surfactant sensing by nematic micro-droplets was reported through boundary change mechanism by Humar et al. [18]. Detection of subtle phase transition among liquid crystal mesophases has also been demonstrated from the WGM study [19]. Yan Wang et al. have studied the dye doped cholesteric liquid crystals micro-droplet based microcavities [20]. Recently, we have shown temperature, magnetic and electric field tuning of structure and WGM resonance in nematic and ferromagnetic nematic droplets [21,22]. In most of the previous studies either glycerol or polydimethylsiloxane (PDMS) were used as supporting media. It was reported that the micro-droplets in these dispersing media are not stable in the sense that the diameter decreases slowly with time [22]. This is disadvantageous as far as the application point of view is concerned and, hence, it is important to find a suitable supporting media with desired properties. In this article, we report experimental studies on several polymer and liquid crystal systems. We find that the size of liquid

crystal micro-droplets is most stable with time in a low refractive index, highly transparent perfluoropolymer solution. The electric field creates a substantial elastic distortion in the micro-droplets of a negative dielectric anisotropy nematic liquid crystal but the resonance properties remain unaffected and this is in contrast to the results reported in droplets of positive dielectric anisotropy liquid crystals. We report quality factor, $Q \simeq 1.2 \times 10^4$ in our system, which is so far the highest reported value in liquid crystal based microresonators.

2. Experimental

In the experiment, we have used two liquid crystals namely, pentyl cyano biphenyl (5CB) and a negative dielectric anisotropy nematic liquid crystal mixture, MLC-6608. 5CB was obtained from Sigma-Aldrich and it exhibits room temperature nematic phase. MLC-6608 was obtained from Merck and it exhibits a wide temperature range of nematic phase, extending from -30°C to 90°C . The dielectric anisotropy of MLC-6608 is negative, i.e. $\Delta\epsilon = -4.2$ and the elastic constants at ambient temperature are; $K_{11} = 16.7 \times 10^{-12}\text{N}$, $K_{22} = 7.0 \times 10^{-12}\text{N}$ and $K_{33} = 18.1 \times 10^{-12}\text{N}$, respectively [23,24]. Since both of them are room temperature nematic liquid crystals, all the experiments are performed at ambient temperature. The extraordinary and ordinary refractive indices of 5CB at room temperature are given by $n_e = 1.702$ and $n_o = 1.55$ [25]. In case of MLC-6608, $n_e = 1.56$ and $n_o = 1.477$ [26]. We used three polymers as supporting media namely, PDMS, a mixture of glycerol-lecithin and a perfluoropolymer, i.e. poly(perfluoro (4-vinyl-1-butene)), commonly known as CYTOP (CTX-809A). CYTOP was obtained from Asahi Glass Co. Ltd, Japan. We prepared a solution with volumetric ratio 2:1 of CT-Sol.180 solvent

and CTX-809A. The refractive index of PDMS and glycerol are 1.38 and 1.47, respectively [27]. PDMS provides homeotropic whereas glycerol provides planar liquid crystal anchoring. A small amount of lecithin (about 5 to 10 wt %) mixed with glycerol provides homeotropic anchoring. The refractive index of CYTOP is 1.34 and is much smaller than that of both PDMS and glycerol. CYTOP is highly transparent over a wide wavelength range (200 nm to 2 μ m) and is used as an antireflective coating in organic light emitting devices [28,29]. It has high solubility in perfluorinated solvents and is highly resistant to chemical and thermal stimuli [30]. It has been used as an alignment layer for liquid crystals and several experiments showing the discontinuous anchoring transition have been reported [30–39]. Micrometre size droplets were dispersed through micropipette injection in the supporting media. About 1 to 2 μ L of liquid crystal was injected into 1000 μ L of polymer and the tip of the micropipette was moved in a circular fashion while releasing in to the polymer. This protocol provides well separated micro-droplets with definite structure dispersed in the polymer. The micro-droplets are highly stationary inside the polymers and no sedimentation is observed during the experiment. Prior to the droplet formation, the liquid crystals were doped with 0.1 to 0.5% of Nile red fluorescent dye. No curing agent was added to the polymers because it often changes the surface anchoring of the liquid crystals. The wavelength of Argon-ion laser (514 nm) falls in the excitation band of Nile red and the fluorescence emission from the sample is observed within a range of 540–700 nm.

In the electric field experiments, we placed the supporting media containing liquid crystal micro-droplets between two indium-tin-oxide-coated (ITO) glass plates with appropriate spacers. Micro-droplets with uniform radial director structure were selected and excited with a focussed beam of Argon-ion laser (514 nm) through the objective of the microscope. The light emitted by the dye-doped droplets is collected by the same objective and is sent to the spectrometer (Andor 500i) which is connected to the inverted polarising microscope (Nikon, Eclipse Ti-U) [22]. Sinusoidal voltage was applied across the cell with the help of a function generator (Tektronix-AFG 3102) fixed at 5 KHz frequency and a voltage amplifier (TEGAM-2350).

3. Results and discussion

We studied the time dependent size of the micro-droplets using a polarising optical microscope (POM). Figure 2 shows the time variation of diameters of a few 5CB micro-droplets in PDMS (Figure 2(a)) and in glycerol (90%) lecithin (10%) mixture (Figure 2(b)). 5CB in PDMS shows a radial anchoring whereas in

pure glycerol it shows planar anchoring with a pair of boojum defects situated diametrically opposite. We find that a small amount of lecithin in glycerol induced homeotropic anchoring with radial director structure. In PDMS, the micro-droplet diameter decreases rapidly in a nonlinear way. For example the diameter of 70 μ m droplet decreases nearly to 10 μ m within 2 h (Figure 2(a)). In fact sometimes the micro-droplets disappear completely over a long period of time. An empirical equation; $D(t) = D(0) + Ae^{-t/\tau}$, is fitted to get the decay constant for a particular droplet, where A is a constant. The decay constant $\tau \simeq 50$ min, suggesting 63% of the size is shrunken within 50 min after the droplet formation. In case of glycerol-lecithin mixture, the micro-droplet diameter decreases linearly but it is much slower than PDMS (Figure 2(b)). For example, the diameter of a 26 μ m droplet decreases to about 21 μ m after about 6 h. Beyond about 50 min the micro-droplet size decreases by about 100 nm/min. For bigger droplets ($D > 40 \mu$ m), initially the decay is faster (about 350 nm/min) and there is a clear slope change at about 30 min. Therefore, glycerol lecithin mixture is comparatively better dispersing medium than PDMS for WGM experiments. However, the glycerol-lecithin mixture appears yellowish and the scattering as well as absorption losses are relatively higher than PDMS. These shortcomings motivated us to look for an alternative supporting medium.

There are some studies reporting the alignment properties of liquid crystals on CYTOP solution [31–33]. We have chosen it as a supporting medium for studying the liquid crystal micro-droplets. Figure 3(a) shows micro-droplets of MLC-6608 liquid crystal dispersed in CYTOP solution. It stabilises spherical micro-droplets with radial anchoring. Four orthogonal dark brushes with concentric rings around the centre suggest the director is orthogonal to the interface and radially symmetric. A radial hedgehog point defect is seen at the centre of the droplets. Figure 3(b) shows the variation of diameter of a few micro-droplets with time at room temperature, measured using optical microscope. It is observed that micro-droplet diameter decreases very slowly with time and beyond about 3 h of formation, they are completely stabilised (time shown by dotted line in Figure 3(b)). Thus, CYTOP solution is much better supporting medium than PDMS and glycerol-lecithin mixtures at ambient temperature. The CYTOP has a large number of fluorine atoms. Fluorine has a small atomic radius and the largest electronegativity among the atoms, so that it forms a stable covalent bond with carbon and is effective in lowering the surface energy. Hence, liquid crystal molecules are not soluble in CYTOP solution [37] owing to the high bonding energy of C-F (485 kJ mol⁻¹) and C-C (360 kJ mol⁻¹) bonds [40].

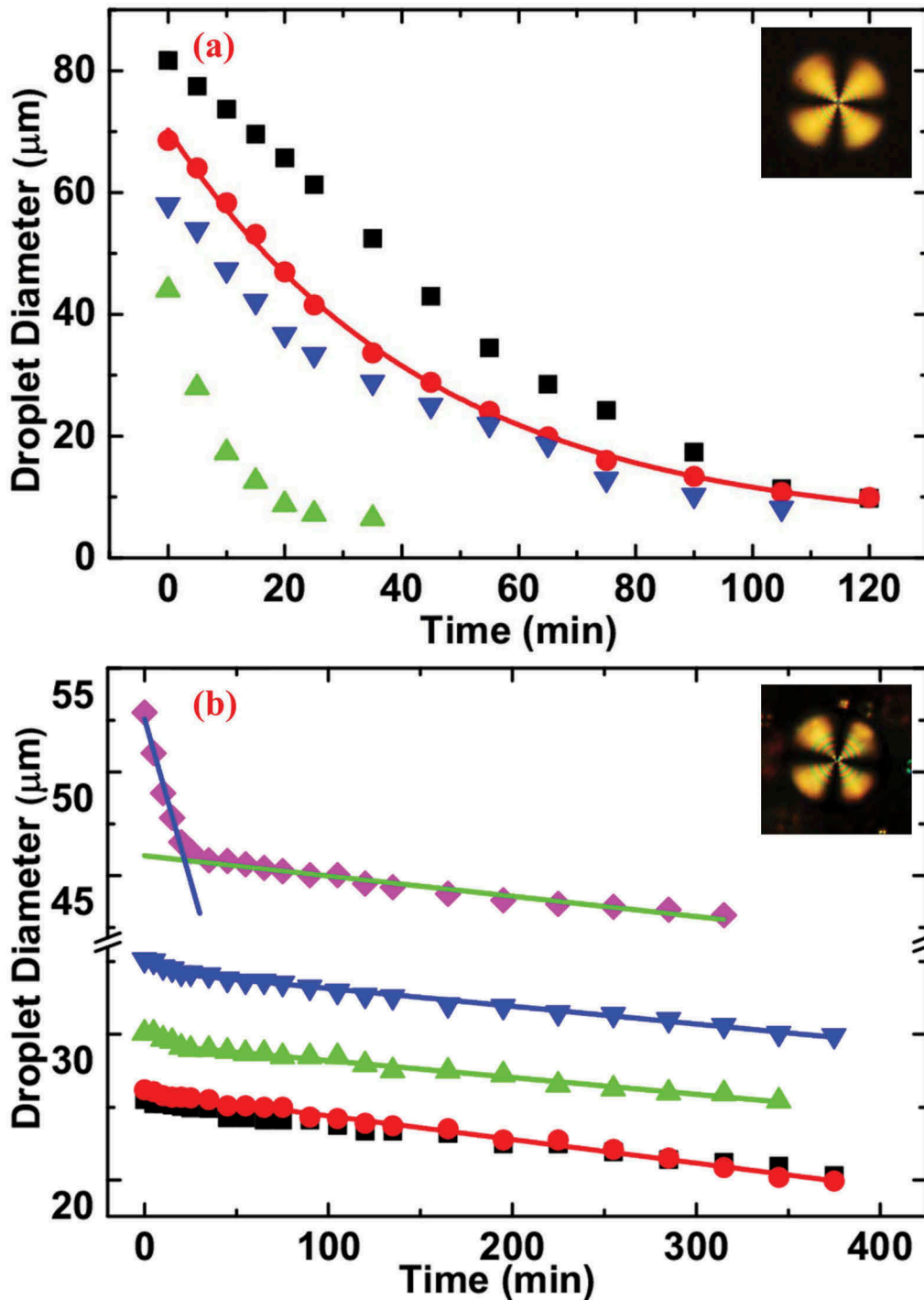


Figure 2. (Colour online) Variation of diameter of 5CB micro-droplets with time dispersed in (a) PDMS (b) glycerol (90%) lecithin (10%) mixture. Different colours represent LC micro-droplets with different initial diameters and their time evolution. The continuous red line in (a) is a best fit to the equation; $D(t) = D(0) + Ae^{-t/\tau}$. Continuous lines in (b) are linear best fits. The measurements are made directly from the optical microscope at room temperature. (Inset) Polarising optical microscope images of micro-droplets with defects.

We selected a micro-droplet of MLC-6608 of diameter $10.6 \mu\text{m}$ for studying optical resonance. [Figure 4\(a\)](#) shows the polarising optical microscope image. [Figure 4\(b\)](#) shows spherical micro-droplet with sharp interface of the droplet-CYTOP solution. [Figure 4\(c\)](#) shows excitation of WGM in the dye doped micro-

droplet when illuminated by a tightly focused 514 nm laser beam through a $60\times$ objective. A light strip running diametrically across the droplet suggests the localisation of the modes around it. [Figure 4\(d\)](#) shows a typical WGM resonance spectrum. The resonance modes are observed on the overlay of the

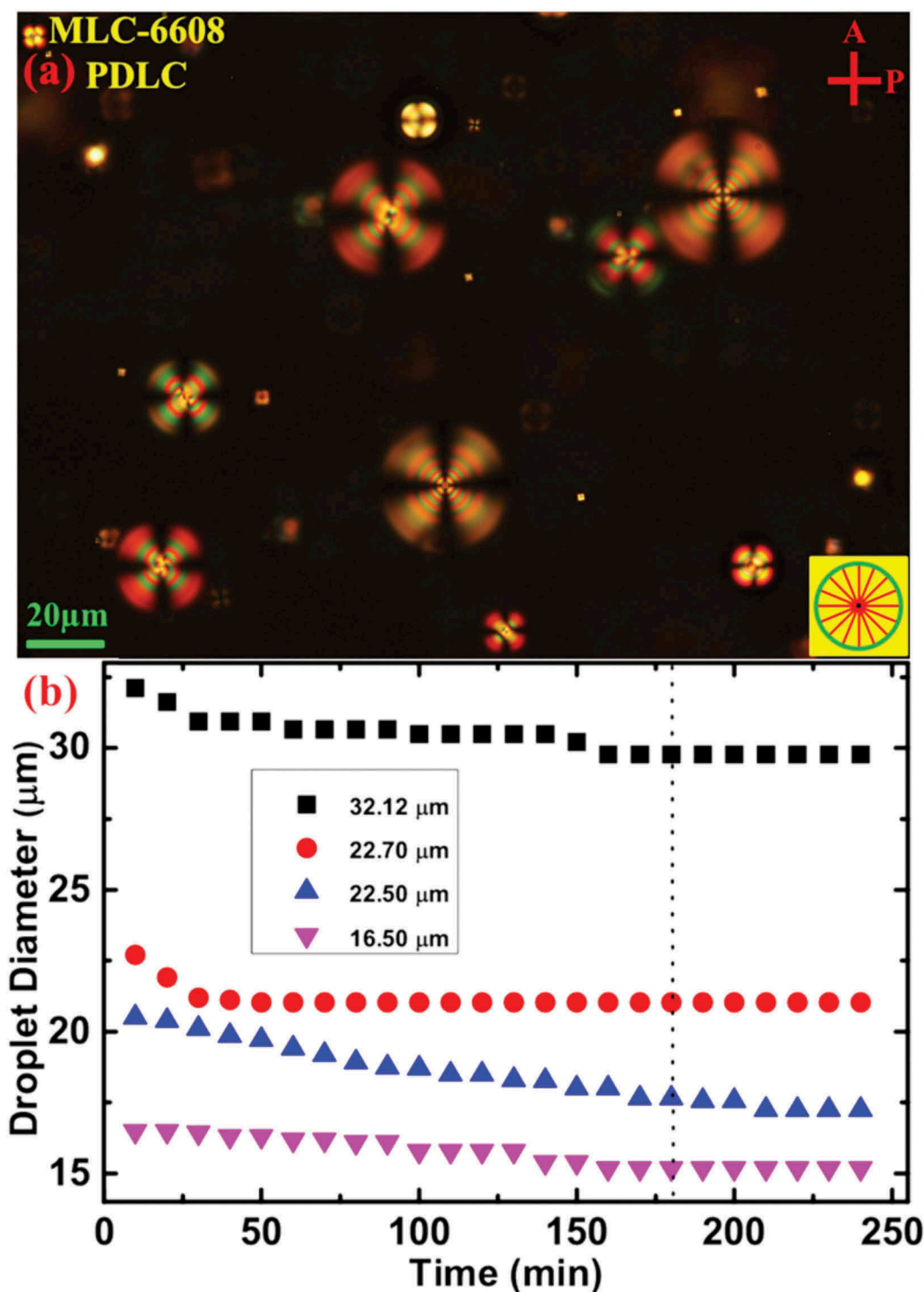


Figure 3. (Colour online) (a) Polarising optical microscope images (POM) of MLC-6608 micro-droplets of various size suspended in CYTOP solution. Inset shows a schematic diagram of radial director structure (b) Variation of micro-droplet diameters with time at room temperature measured by using optical microscope. Different colours represent LC micro-droplets with different initial diameters and their time evolution. The vertical dotted line indicates the time beyond which the droplets are highly stable and used for optical resonance studies.

fluorescence intensity of the droplet. Liquid crystals are birefringent and, hence, possess different refractive indices for different polarisations. In transverse magnetic mode (TM), the electric field oscillates along the

longer molecular axes while as in transverse electric mode (TE), the electric field oscillates perpendicular to it. In spherical micro-droplets, the refractive index sensed by former polarisation is extraordinary index

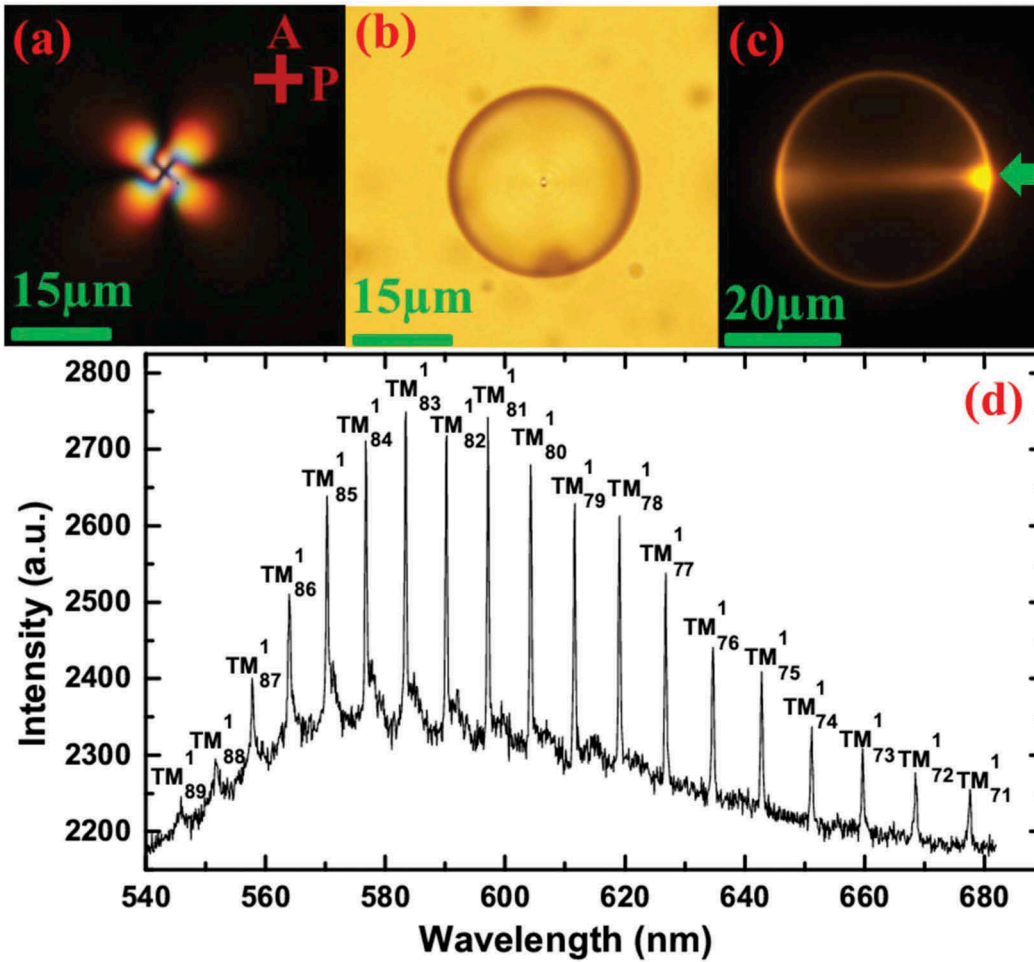


Figure 4. (Colour online) (a) Optical polarising micrograph of an MLC-6608 micro-droplet dispersed in CYTOP solution at room temperature. (b) Droplet as seen without polarisers. (c) A Nile-Red dye-doped micro-droplet illuminated by a focussed 514 nm laser beam. The irradiation point is marked by green arrow. (d) Optical resonance spectrum recorded by the spectrometer from an illuminated micro-droplet with calculated TM modes.

(n_e) and the latter one experiences ordinary index (n_o). Using analytical solutions of Mie type theories, the resonant frequencies for spherical birefringent micro-resonators can be calculated [12]. It has been shown that for the TE mode in the radial anisotropic micro-sphere is equivalent to the TE mode in an isotropic microsphere with the ordinary refractive index, whereas the TM mode couples to both the ordinary and extraordinary refractive indices. However, for a spherical resonator with small radial mode numbers q the resonant WGM frequencies can be obtained analytically [41]. For a droplet of diameter $10.6 \mu\text{m}$, we find that only TM modes with radial mode number $q = 1$ are supported. The angular mode numbers (l) for the same droplet are calculated using $n_s = 1.557$ [42] and $n_a = 1.34$ [37]. In the wavelength range of 540–680 nm, l varies from 71 to 89, which is labelled in Figure 4(d).

The stability of the droplets was further studied by measuring the free spectral range (FSR). It is defined as:

$$FSR = \delta\lambda_{SM} = \frac{\lambda^2}{n_{eff}\pi D} \quad (1)$$

where, $1/n_{eff}^2 = \sin^2\theta/n_e^2 + \cos^2\theta/n_o^2$ and $\delta\lambda_{SM}$, D , n_e , n_o and θ are spacing between two successive modes, the diameter of the micro-droplets, extraordinary refractive index, ordinary refractive index of the liquid crystal and the angle between the optical axis and the light propagation direction, respectively [43]. Figure 5(a) shows the variation of FSR with time for a few micro-droplets. The measurements were made after 3 h from the formation of the droplets. It is observed that the FSR for all the micro-droplets is independent of time. Figure 5(b) shows the variation of FSR for several

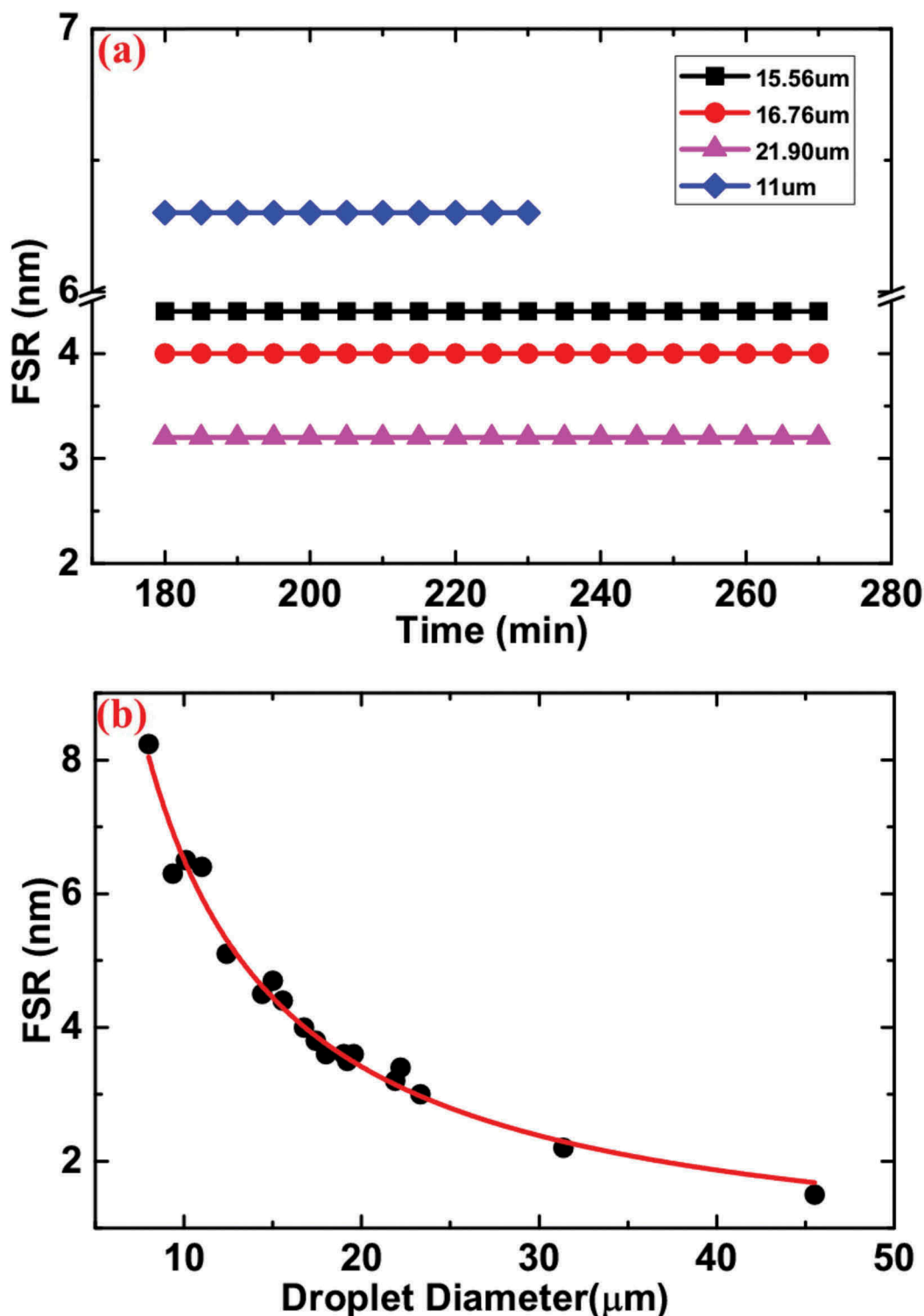


Figure 5. (Colour online) (a) Time dependence of FSR of different size microdroplets dispersed in CYTOP solution. (b) Variation of FSR with droplet size. The red line is the best fit to $FSR \propto 1/D$. The error bar in (a) is almost equal to the point size. All the measurements are made at room temperature.

micro-droplets with varying diameter from 7 to 45 μm. The FSR is inversely proportional to the droplet diameter (D). The best fit to the data ($FSR \propto 1/D$) is also shown in Figure 5(b).

The WGMs displayed by the micro-droplets are highly morphology dependent. In case of liquid crystals the director inside the droplets is distorted by external electric and magnetic fields and consequently WGM resonance

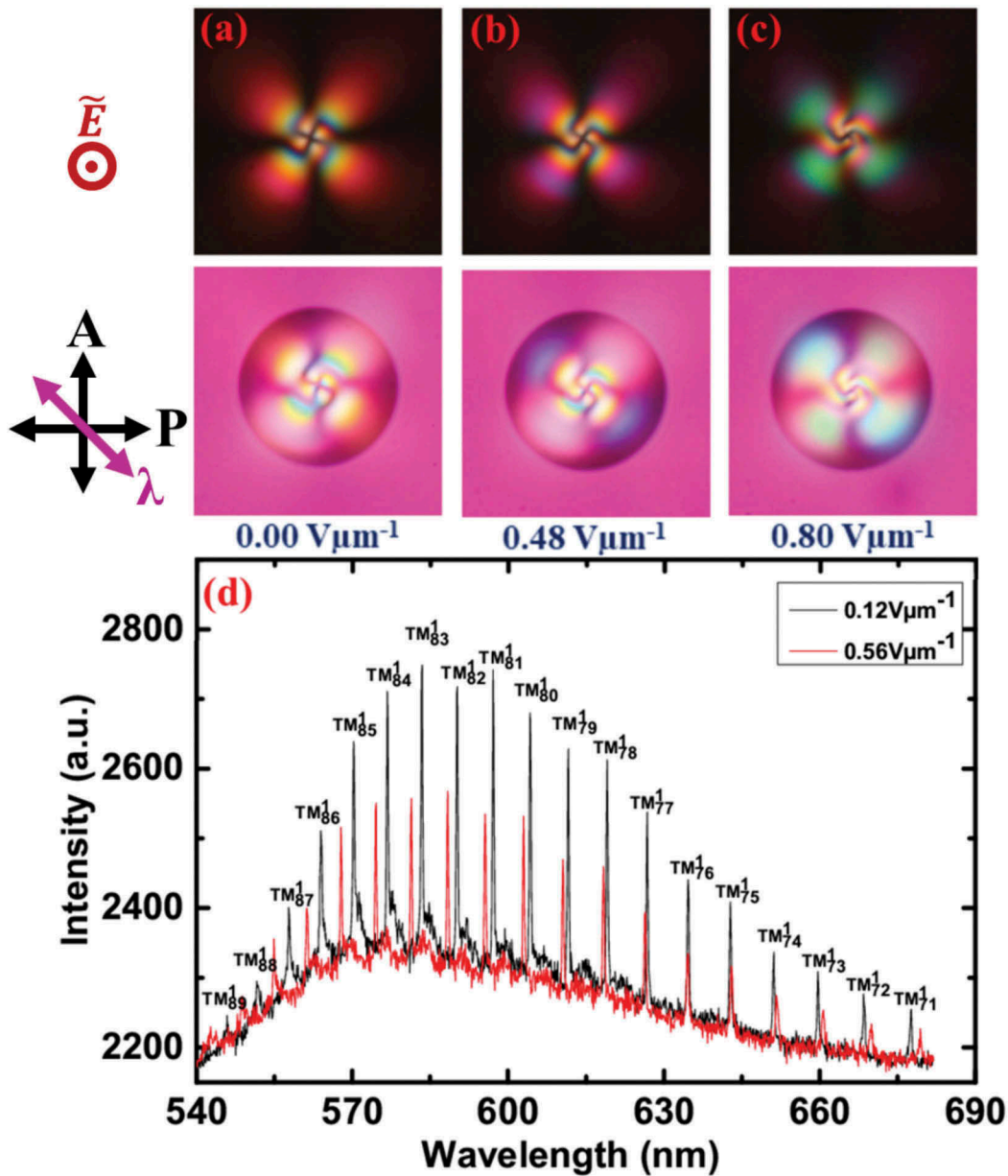


Figure 6. (Colour online) Optical polarising micrographs of elastic distortion of a microdroplet dispersed in CYTOP solution at (a) zero electric field (b-c) increasing electric field. Corresponding λ -plate images are shown underneath. (d) Representative WGM spectra of a droplet below ($0.12 \text{ V}/\mu\text{m}$) and above ($0.56 \text{ V}/\mu\text{m}$) Freedericksz threshold field. The direction of electric field and the orientation of the slow axis of the λ -plate with respect to the crossed polarisers is shown on the left side.

properties are expected to get affected. In our previous studies we showed the effect of electric field on the WGM resonance properties of a liquid crystal exhibiting positive dielectric anisotropy ($\Delta\epsilon > 0$) [22]. In the present experiment the dielectric anisotropy of MLC-6608 is negative ($\Delta\epsilon < 0$). The effect of electric field on the micro-droplets and defects in liquid crystal micro-droplets with $\Delta\epsilon < 0$ has been studied [44], however, its subsequent effects on the resonance properties have not been studied so far. Figure 6 (a-c) shows typical elastic distortion in a micro-droplet when applied electric field is parallel to the direction of light propagation ($E \parallel k$). The director configuration is

mostly radial with a slight azimuthal twist near the central region that encompasses a radial hedgehog defect. The structure becomes complex with increasing field and the distortion from the central region expands towards the boundary (see λ -plate image). It has been suggested that the hedgehog defect undergoes a continuous transition into an escape non-singular line defect with $s = 1$ [44]. It appears that the line defect is well within the central region and no significant or noticeable distortion of the director is observed very close to the inner boundary wall. The WGM spectra of a $10.6 \mu\text{m}$ droplet at two representative fields namely $0.12 \text{ V}/\mu\text{m}$ and $0.56 \text{ V}/\mu\text{m}$ are shown in Figure 6

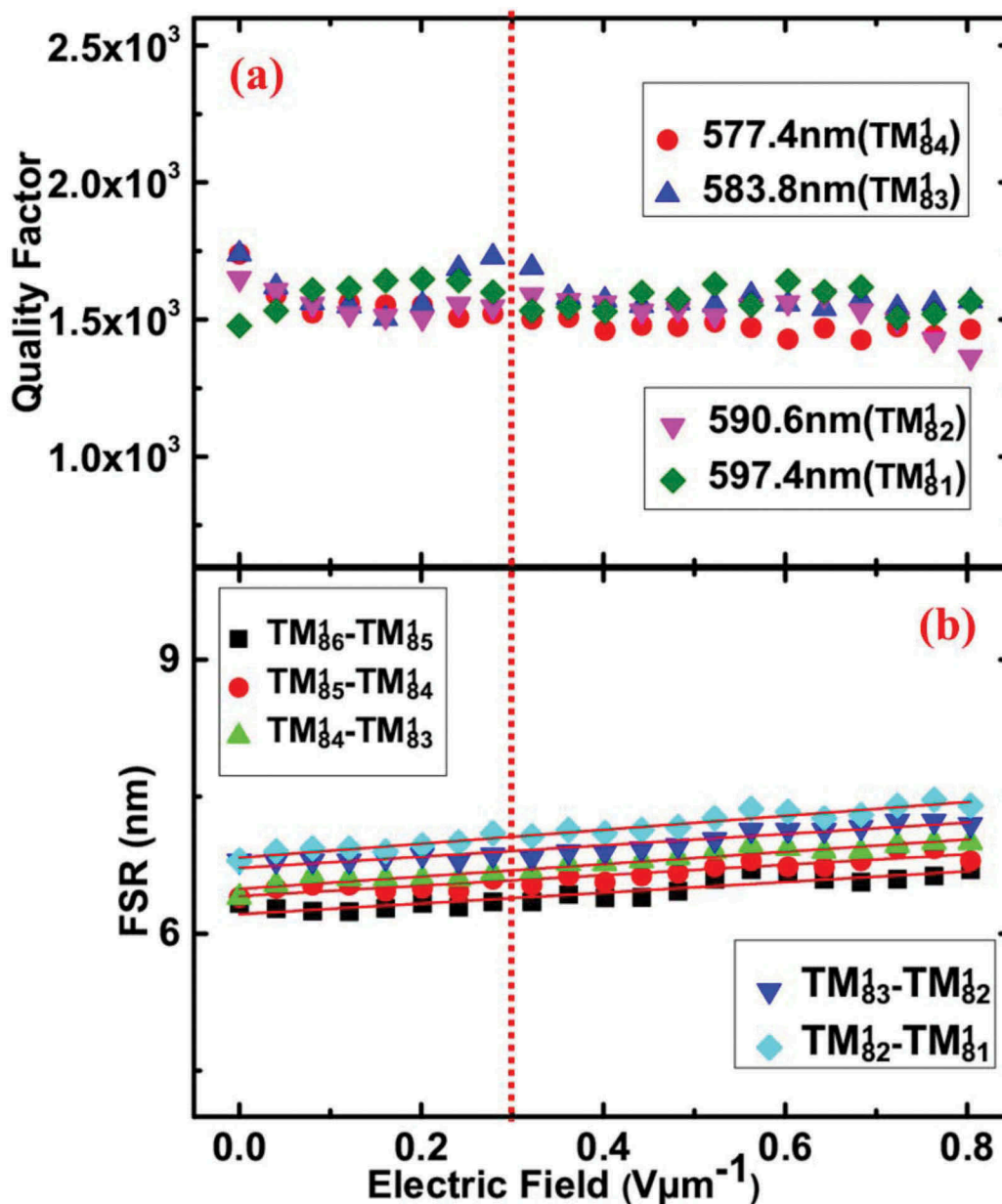


Figure 7. (Colour online) (a) Variation of Q-factor ($\lambda/\Delta\lambda$) of a few TM modes with applied electric field of an MLC-6608 microdroplet with diameter $10.7 \mu\text{m}$ dispersed in CYTOP solution. Grating used 300 lines/mm. (b) Variation of FSR with applied electric field of a few TM modes. Vertically dotted line represents the Fredericksz threshold field.

(d). The resonance intensity decreases slightly with increasing field. The modes above 635 nm shift slightly towards higher wavelength and below, they shift towards lower wavelength side.

We measured the Q-factor and FSR at different fields of a few modes. It is defined as: $Q = \lambda/\Delta\lambda$, where $\Delta\lambda$ is the full-width at half maxima of a mode. Figure 7(a,b) shows field dependent Q-factor and FSR. We used a grating of 300 lines/mm (spectral resolution 0.32 nm) to observe and analyse many modes over a larger wavelength range. It is observed that Q-factor is about 1.5×10^3 and remains almost unchanged with

applied electric field. This is in sharp contrast with the resonance properties of micro-droplets with $\Delta\epsilon > 0$, where a substantial decrease in Q was reported beyond Fredericksz threshold field [22]. The Fredericksz threshold field for MLC-6608 is about $0.3 \text{ V}/\mu\text{m}$. This means that just inside the liquid crystal-CYTOP boundary where the light is circulating there is no elastic deformation. In other words, the circulating light is confined within the extrapolation length inside the interface. This is consistent with the observation (see λ -plate images in Figure 6), where the elastic distortion is mostly confined near the central region.

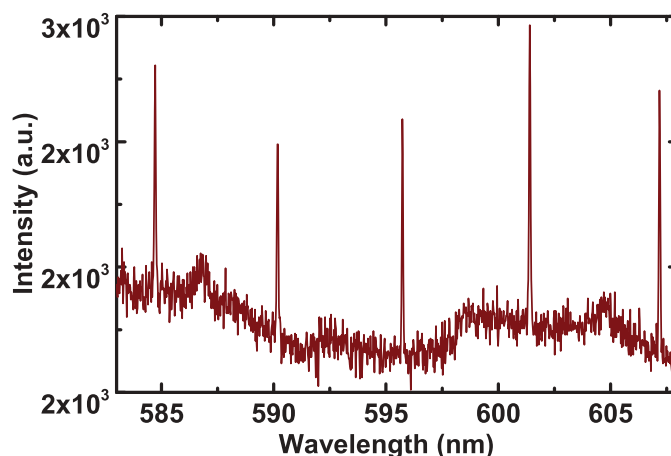


Figure 8. (Colour online) Optical resonance spectrum recorded by the spectrometer using a high resolution grating of 2400 lines/mm without any electric field of an MLC-6608 microdroplet in CYTOP solution. Droplet diameter 10.6 μm .

Figure 7(b) shows the variation of FSR with the applied electric field. It is observed that FSR of the modes is about 7 nm and is almost independent of the applied electric field. FSR depends mainly on two parameters namely; the diameter (D) and the effective refractive index (n_{eff}) of the droplet. Thus, both the droplet diameter and the effective refractive index at the interface do not change with the applied electric field.

The CYTOP solution is highly transparent and hence the absorption is very low [37] and in addition, it has lower refractive index than PDMS or glycerol or other polymers reported so far in WGM resonance studies. Hence quality factor is expected to be larger. We used high resolution grating (2400 lines/mm) which gives a spectral resolution of 0.021 nm within a small wavelength range. Figure 8 shows a few highly narrow TM modes of a 10.6 μm droplet. The estimated quality factor of these modes is about $Q \simeq 1.2 \times 10^4$. It is the highest Q-factor reported so far in case of liquid crystal micro-droplets and is larger by about 2000 than the previous report [12].

4. Conclusions

In summary, we find that CYTOP solution is one of the best supporting media for forming stable liquid crystal micro-droplets, which is very crucial for the successful realisation of liquid crystal based microresonators. This is the first optical resonance study on negative dielectric anisotropy liquid crystal micro-droplets. FSR is inversely proportional to the diameter of the micro-droplets in accordance with the prediction and, hence, smaller micro-droplets are of greater importance. The circulating light is confined within the extrapolation length at the boundary region where the resonant modes are located. Consequently the quality factor remains unaffected inspite

of elastic distortion in the micro-droplets by the external electric field. The highest quality factor is attributed to the low refractive index and high transparency of the supporting medium CYTOP solution. Finally, we showed a new application of CYTOP solution in liquid crystal based microresonators with superior performance. The resonance properties, when the applied electric field parallel to the direction of exciting laser beam are not encouraging for electrical tuning of the resonance. The in-plane electric field, i.e. the field direction perpendicular to the director is expected to be more effective but further studies are required.

Acknowledgments

J.A.S acknowledges UGC for BSR fellowship.

Disclosure statement

No potential conflict of interest was reported by the authors.

Funding

We gratefully acknowledge the support from SERB [EMR/2015/001566] and DST [DST/SJF/PSA-02/2014-2015].

ORCID

Surajit Dhara  <http://orcid.org/0000-0003-3144-0300>

References

- [1] Drzaic PS. Liquid crystals dispersion. Singapore: World Scientific; 1995.
- [2] Prasad PN, Mark JE, Fai TJ. Polymers and other advanced materials. Boston, MA: Springer; 1995.

- [3] Coates D. Polymer-dispersed liquid crystals, *J Mater Chem.* **1995**;5:2063.
- [4] Loudet JC, Barois P, Poulin P. Colloidal ordering from phase separation in a liquid-crystalline continuous phase. *Nature.* **2000**;407:611.
- [5] De Gennes PG, Prost J. *The physics of liquid crystals.* New York: Oxford University; **1993**.
- [6] Lavrentovich OD. Topological defects in dispersed words and worlds around liquid crystals, or liquid crystal drops. *Liq Cryst.* **1998**;24:117.
- [7] Porenta T, Ravnik M, Zumer S. Effect of flexoelectricity and order electricity on defect cores in nematic droplets. *Soft Matter.* **2011**;7:132.
- [8] Zhou Y, Bukusoglu E, Martínez-González JA, et al. Structural transitions in cholesteric liquid crystal droplets. *ACS Nano.* **2016**;10:6484.
- [9] Urbanski M, Reyes CG, Noh J, et al. Liquid crystals in micron-scale droplets, shells and fibers. *J Phys Condens Matter.* **2017**;29:133003.
- [10] Posnjak G, Copar S and Musevic I. Hidden topological constellations and polyvalent charges in chiral nematic droplets. *Nat Commun.* **2017**;8:14594.
- [11] Yoshioka J, Araoka F. Topology-dependent self-structure mediation and efficient energy conversion in heat-flux-driven rotors of cholesteric droplets. *Nat Commun.* **2018**;9:432.
- [12] Humar M, Ravnik M, Pajk S, et al. Electrically tunable liquid crystal optical microresonators. *Nat Photon.* **2009**;3:595.
- [13] Humar M, Musevic I. 3D microlasers from self-assembled cholesteric liquid-crystal microdroplets. *Opt Express.* **2010**;18:26995.
- [14] Humar M. Liquid-crystal-droplet optical microcavities. *Liq Cryst.* **2016**;43:1937.
- [15] Yang S, Ta VD, Wang Y, et al. Reconfigurable liquid whispering gallery mode microlasers. *Sci Rep.* **2016**;6:27200.
- [16] Vahala K. *Optical microcavities.* Singapore: World Scientific; **2004**.
- [17] Arnold S, Holler S, Druger SD. Optical processes in micro-cavities. In: editors, Chang RK, Campillo AJ. *Advanced series in applied physics.* Vol. 3. Singapore: World Scientific; **1996**.
- [18] Humar M, Musevic I. Surfactant sensing based on whispering-gallery-mode lasing in liquid-crystal microdroplets. *Opt Express.* **2011**;19:19836.
- [19] Kumar TA, Mohiddon MA, Dutta N, et al. Detection of phase transitions from the study of whispering gallery mode resonance in liquid crystal droplets. *Appl Phys Lett.* **2015**;106:051101.
- [20] Zhao L, Wang Y, Li H, et al. Tunable whispering gallery modes lasing in dye-doped cholesteric liquid crystal microdroplets. *Appl Phys Lett.* **2016**;109:231906.
- [21] Marusa M, Sofi JA, Kvasić I, et al. Magnetic-field tuning of whispering gallery mode lasing from ferromagnetic nematic liquid crystal microdroplets. *Opt Express.* **2017**;25:1073.
- [22] Sofi JA, Mohiddon MA, Dutta N, et al. Electrical and thermal tuning of quality factor and free spectral range of optical resonance of nematic liquid crystal microdroplets. *Phys Rev E.* **2017**;96:022702.
- [23] Nie X, Lin YH, Wu ST. Polar anchoring energy measurement of vertically aligned liquid-crystal cells. *J Appl Phys.* **2005**;98:013516.
- [24] Li Jun. *Refractive Indices Of Liquid Crystals And Their Applications In Display And Photonic Devices.* **2005**. Electronic Theses and Dissertations. 4460. University of Central Florida. <http://stars.library.ucf.edu/etd/4460>
- [25] Horn RG. Refractive indices and order parameters of two liquid crystals. *J De Physique.* **1978**;39:105–109.
- [26] Li J, CbH W, Gauza S, et al. Refractive Indices of liquid crystals for display applications. *J Disp Technol.* **2005**;1:1.
- [27] Hoyt LF, Buffalo NY. New table of the refractive index of pure glycerol at 20C. *J Ind Eeg Chem.* **1934**;26:329.
- [28] Yamamoto K, Ogawa G. Structure determination of the amorphous perfluorinated homopolymer: poly[perfluoro(4-vinyloxy-1-butene)]. *J Fluorine Chem.* **2005**;126:1403.
- [29] Jeong SM, Araoka F, Machida Y, et al. Enhancement of normally directed light outcoupling from organic light-emitting diodes using nanoimprinted low-refractive-index layer. *Appl Phys Lett.* **2008**;92:083307.
- [30] Kim JK, Jeong SM, Dhara S, et al. Bistable device using anchoring transition of nematic liquid crystals. *Appl Phys Lett.* **2009**;95:063505.
- [31] Kumar TA, Takezoe H, Dhara S. Perfluoropolymer as planar alignment layer for liquid crystal mixtures. *Jpn J Appl Phys.* **2011**;50:040203.
- [32] Kumar TA, Sastry VSS, Ishikawa K, et al. Effect of an electric field on defects in a nematic liquid crystal with variable surface anchoring. *Liq Cryst.* **2011**;38:971.
- [33] Kumar TA, Le KV, Aya S. Anchoring transition in a nematic liquid crystal doped with chiral agents. *Phase Transitions.* **2012**;85:888.
- [34] Jampani VSR, Skarabot M, Takezoe H, et al. Laser-driven microflow-induced bistable orientation of a nematic liquid crystal in perfluoropolymer-treated unrubbed cells. *Opt Express.* **2013**;21:724.
- [35] Rasna MV, Zuhail KP, Manda R, et al. Discontinuous anchoring transition and photothermal switching in composites of liquid crystals and conducting polymer nanofibers. *Phys Rev E.* **2014**;89: 052503.
- [36] Dhara S, Kim JK, Jeong SM, et al. Anchoring transitions of transversely polar liquid-crystal molecules on perfluoropolymer surfaces. *Phys Rev E.* **2009**;79:060701.
- [37] Jeong SM, Shimbo Y, Araoka F, et al. Perfluoropolymer surface for shock-free homeotropic alignment of smectic liquid crystals. *Adv Mater.* **2010**;22:34.
- [38] Sai DV, Kumar TA, Haase W, et al. Effect of smectic short-range order on the discontinuous anchoring transition in nematic liquid crystals. *J Chem Phys.* **2014**;141:044706.
- [39] Kumar TA, Sathyanarayana P, Sastry VSS, et al. Temperature- and electric-field-induced inverse Freedericksz transition in a nematogen with weak surface anchoring. *Phys Rev E.* **2010**;82:011701.
- [40] Arcella V, Colaianna P, Maccone P, et al. A study on a perfluoropolymer purification and its application to membrane formation. *J Membr Sci.* **1999**;163:203–209.
- [41] Lam CC, Leung PT and Young K. Explicit asymptotic formulas for the positions, widths, and strengths of resonances in Mie scattering. *J Opt Soc Am B.* **1992**;9:1585.
- [42] Scharf T. *Polarized light in liquid crystals.* New Jersey: Wiley Online Library; **2006** April.
- [43] Si G, Zhao Y, Leong E, et al. Liquid-crystal-enabled active plasmonics: a review. *Materials.* **2014**;7(2):1296–1317.
- [44] Xu F, Kitzerow H-S, Crooker PP. Electric-field effects on nematic droplets with negative dielectric anisotropy. *Phys Rev A.* **1992**;46:6535–6540.